

UNCLASSIFIED

AD 4 3 6 8 8 7

DEFENSE DOCUMENTATION CENTER

FOR

SCIENTIFIC AND TECHNICAL INFORMATION

CAMERON STATION, ALEXANDRIA, VIRGINIA



UNCLASSIFIED

NOTICE: When government or other drawings, specifications or other data are used for any purpose other than in connection with a definitely related government procurement operation, the U. S. Government thereby incurs no responsibility, nor any obligation whatsoever; and the fact that the Government may have formulated, furnished, or in any way supplied the said drawings, specifications, or other data is not to be regarded by implication or otherwise as in any manner licensing the holder or any other person or corporation, or conveying any rights or permission to manufacture, use or sell any patented invention that may in any way be related thereto.

**Best
Available
Copy**

WADD-TR-61-94
Part III

TOTAL NORMAL AND TOTAL HEMISPHERICAL EMITTANCE
OF POLISHED METALS - PART III

TECHNICAL REPORT NO. WADD-TR-61-94, Part III

December 1963

AF Materials Laboratory
Research and Technology Division
Air Force Systems Command
Wright-Patterson Air Force Base, Ohio

Project 7360, Task 736001

(Prepared under Contract No. MIPR 33(657)-2-RD-155 by the U. S. Naval
Radiological Defense Laboratory, San Francisco, California; G. L.
Abbott, author)

436887

64-12

436887

NO COPY

1.00

NOTICES

When Government drawings, specifications, or other data are used for any purpose other than in connection with a definitely related Government procurement operation, the United States Government thereby incurs no responsibility nor any obligation whatsoever; and the fact that the Government may have formulated, furnished, or in any way supplied the said drawings, specifications, or other data, is not to be regarded by implication or otherwise as in any manner licensing the holder or any other person or corporation, or conveying any rights or permission to manufacture, use, or sell any patented invention that may in any way be related thereto.

Qualified requesters may obtain copies of this report from the Defense Documentation Center (DDC), (formerly ASTIA), Cameron Station, Bldg. 5, 5010 Duke Street, Alexandria 4, Virginia

This report has been released to the Office of Technical Services, U.S. Department of Commerce, Washington 25, D.C., for sale to the general public.

Copies of this report should not be returned to the Aeronautical Systems Division unless return is required by security considerations, contractual obligations, or notice on a specific document.

FOREWORD

This report was prepared by the U. S. Naval Radiological Defense Laboratory under USAF Contract MIPR 33(657)-2-RD-155. The work was performed under Project No. 7360, "The Chemistry and Physics of Materials", Task No. 736001, "Thermodynamics and Heat Transfer". The work was administered under the direction of the AF Materials Laboratory, Research and Technology Division, with Raymond J. Prezecki acting as project engineer.

This report covers work conducted from 27 February 1962 to 19 December 1962.

ABSTRACT

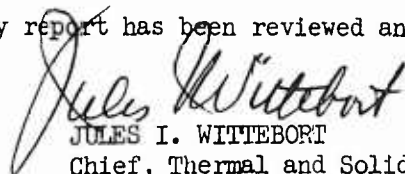
The total hemispherical emittance, the total normal emittance, and the variation of electrical resistivity with temperature were measured on aged surfaces of tantalum, niobium, and tungsten in a vacuum over a temperature range from 1000°K to 3000°K (subject to the material). In addition, the normal spectral emittance at 0.65 micron was measured on tantalum and niobium. The total hemispherical emittance was obtained from the measured power dissipation within the uniform temperature region at the center of an electrically heated ribbon; its temperature being measured with a thermocouple or an optical pyrometer when the spectral emittance was known. The total normal emittance was determined by using a radiation thermopile. The ratio of total hemispherical to total normal emittance was also calculated directly from the angular distribution of radiation obtained by revolving the ribbon within the field of view of the thermopile. Some data are also included on molybdenum from a previous report.

The total hemispherical emittance was found to be on the average about 20 percent higher than the total normal emittance on tantalum, niobium, and tungsten. The spectral emittance at 0.65 micron for tantalum, niobium, and tungsten is nearly identical from 1000°K to the evaporation limit. The total hemispherical emittance of molybdenum, tantalum, niobium, and tungsten may be represented to within ±5 percent of the measured value by the empirical equation:

$$\epsilon_H = 0.1069 \left(\frac{T}{1000} \right)^{1.21} - 0.000926 \left(\frac{T}{1000} \right)^{4.25}$$

where T is the temperature in degrees Kelvin.

This technical documentary report has been reviewed and is approved.



JULES I. WITTEBORT
Chief, Thermal and Solid State Branch
Materials Physics Division
AF Materials Laboratory

TABLE OF CONTENTS

	PAGE
INTRODUCTION.....	1
BACKGROUND.....	2
PRINCIPLES OF THE EXPERIMENTAL METHOD.....	4
EXPERIMENTAL ARRANGEMENT.....	7
TEMPERATURE DETERMINATION.....	9
RESULTS.....	11
<u>Tantalum</u>	11
<u>Niobium</u>	12
<u>Tungsten</u>	12
DISCUSSION.....	13
REFERENCES.....	16

LIST OF ILLUSTRATIONS

FIGURE		PAGE
1	Detailed Photograph of Experimental Apparatus.....	17
2	Over-all Photograph of Experimental Apparatus.....	18
3	Calibration Curve of Thermopile.....	19
4	Tantalum - Total Hemispherical and Total Normal Emittance.....	19
5	Tantalum - Ratio of Total Hemispherical to Total Normal Emittance.....	20
6	Tantalum - Normal Spectral Emittance at 0.65 Micron.....	20
7	Tantalum - Electrical Resistivity.....	21
8	Niobium - Total Hemispherical and Total Normal Emittance.....	22
9	Niobium - Ratio of Total Hemispherical to Total Normal Emittance.....	22
10	Niobium - Normal Spectral Emittance at 0.65 Micron.....	23
11	Niobium - Electrical Resistivity.....	23
12	Tungsten - Total Hemispherical and Total Normal Emittance.....	24
13	Tungsten - Ratio of Total Hemispherical to Total Normal Emittance.....	24
14	Tungsten - Electrical Resistivity.....	25
15	Molybdenum - Angular Distribution of Radiation versus Angle from Normal.....	26
16	Molybdenum - Angular Distribution of Radiation versus Cosine of Angle from Normal.....	26
17	Total Hemispherical Emittance of Molybdenum, Tantalum, Niobium, and Tungsten.....	27
18	Ratio of Total Hemispherical to Total Normal Emittance of Molybdenum, Tantalum, Niobium, and Tungsten.....	27
19	Ratio of Total Hemispherical to Total Normal Emittance versus Total Normal Emittance for Molybdenum, Tantalum, Niobium, and Tungsten.....	28

LIST OF ILLUSTRATIONS

20	Total Hemispherical Emittance of Platinum, Molybdenum, Tantalum, Niobium, and Tungsten versus the Square Root of the Product of Electrical Resistivity and Temperature.....	29
21	Brightness and True Temperature Relationship for Tantalum, Niobium and Tungsten.....	30

INTRODUCTION

The most important parameter of radiant heat transfer associated with a particular surface is the total hemispherical emittance. This is defined as the ratio of the total radiant energy emitted over all angles from a unit area of a surface to the energy emitted over all angles by an equal area of a perfectly black surface at the same temperature. Now, the total normal emittance considers only the total radiation in a small solid angle at the surface normal and there is an increasingly large volume of data presently being accumulated on the total normal emittance of a variety of materials and surfaces. Indiscriminate substitution of these data for those of total hemispherical emittance could lead to serious errors in many heat transfer problems, particularly in the case of polished metals. The equating of these two emittance values is permissible only when the angular distribution of radiation from the surface obeys Lambert's cosine law.

The reliance that can be put upon high temperature emittance data, at the present time, is not very high for several reasons. Emittance measurements are inherently very difficult because high surface temperatures are hard to measure accurately. The purity level of a given material may vary from sample to sample or the surface may not be entirely free of contamination. The topography of the surface may vary as a result of different preparation techniques or because of thermal etching or recrystallization. Finally, the differences may simply depend on whether or not the quantity being measured is identified as the total normal or total hemispherical emittance. The seriousness of the situation just described is evident when one looks at the disagreement in published total emittances reported for the same material as a result of different investigations. Typical of words used which inadequately characterize an emitting surface are "as received," "oxidized," "sandblasted," "polished," etc. It is not possible to quantitatively describe the fundamental emittance properties of a material unless accompanied by exact surface characterization.

The intent of this research is to report emittance data on refractory metals whose surfaces have been prepared in such a way as to approximate as nearly as possible the theoretical optically smooth, opaque, contamination-free surface. From the knowledge gained here, and from future investigations covering a wider variety of materials and surface conditions, it is hoped that existing emissivity theories may be modified to accurately predict radiative heat transfer. With this better understanding one would then be in a more advantageous position for predicting and understanding radiative properties of other surface preparations.

A program was initiated at the U. S. Naval Radiological Defense Laboratory (USNRDL) to measure the total hemispherical and total normal emittance of electrically heated 0.005 in. thick metal ribbons in a vacuum. By measuring the electrical power dissipation at the center of the uniformly heated specimen, and by detecting the power radiated in a small solid angle normal to it with a total radiation thermopile, the total hemispherical and total normal emittance can be measured simultaneously on the same surface. By allowing the specimen to rotate in the field of view of the thermopile, it is possible to measure the angular distribution of radiation, from which the ratio of total hemispherical to total normal emittance can be calculated directly and thus provide a check on the separate emittance determinations.

Similar techniques and apparatus have been used to measure the total normal and total hemispherical emittance of specular surfaces of platinum¹ and molybdenum² above 1000°K. This paper reports the total hemispherical, total normal, and normal spectral ($\lambda = 0.65$ microns) emittance of tantalum, niobium, and tungsten from 1000°K to their evaporation limited temperature. Reported also is a description of the instrumentation and techniques necessary to obtain these data. Considerable attention is devoted to the problem of temperature measurements between 2000°K and 3000°K.

The research covered in this report is a continuation of that presented in WADD-TR-61-94, Parts I and II (Total Normal and Total Hemispherical Emittance of Polished Metals).¹⁻² Much of the background material and many of the details of the experimental technique described in the earlier reports are pertinent to the material covered in this report. However, sufficient detail will be presented here so that one may understand the experiment without reference to the previous volumes.

BACKGROUND

An expression for the total normal emissivity of metals at moderately low temperatures has been derived by Aschkinass³ and modified by Foote.⁴ This theoretical formula derived by Foote and corrected according to the latest value of the second radiation constant, ($C_2 = 1.4388$ cm-degrees),⁵ is

$$\epsilon_N = 0.578 (\rho T)^{1/2} - 0.179 (\rho T) + 0.044 (\rho T)^{3/2} + \dots \quad (1)$$

where T is the absolute temperature in degrees Kelvin and ρ is the resistivity in ohm-cm. Taking the angular distribution of radiation

into account, Davisson and Weeks⁶ have derived an expression for the total hemispherical emissivity of metals.

$$\epsilon_H = 0.754(\rho T)^{1/2} - 0.635(\rho T) + 0.673(\rho T)^{3/2} - 0.610(\rho T)^2 + \dots \quad (2)$$

There is some ambiguity in the third significant figure of the coefficients in equations (1) and (2) related to the current and past values of the first and second radiation constants. There is not sufficient difference to influence comparisons made in this report, however. It is evident from equations (1) and (2) that there is considerable difference between the total hemispherical and total normal emissivity, and, in the limit of zero temperature, the theoretical value of the total hemispherical emissivity of polished metals is 30 percent higher than the total normal emissivity.

The ratio ϵ_H/ϵ_N is calculated from equations (1) and (2) and is compared with experimental data in this report.

In comparing the measured emittances with the theoretical emissivity which was discussed above, it is necessary to reconsider the relationships between the two quantities. The emittance is equal to the emissivity when certain conditions are met. One, the specimen must be opaque. This is not a difficult requirement to meet for metals. Two, the specimen must be free of surface contamination. This can be achieved reasonably well by cleaning and polishing the specimen and performing the measurements in a vacuum or in an inert atmosphere. Even here an adsorbed layer of gas is held at the surface except in the most extreme vacuums. However, it is assumed that this layer is too thin to be of consequence. Three, the crystalline structure and its defects at the surface must be characteristic of the material rather than a product of the surface treatment. This will always be violated to some extent by polishing or rolling. Four, the surface must be optically smooth; once the specimen is adequately polished, it will retain a smooth surface at low temperatures. However, at elevated temperature, recrystallization and thermal etching take place and the specimen appears rough to the eye. Examination of these surfaces under the microscope shows that the crystallites formed are of the order of 100 microns. There is evidence that these recrystallized surfaces have a slightly higher emittance than the polished surface.² It was found during the present research that other factors tended to have a higher influence on the measured emittance than the recrystallization. Some of these will be described later. Consequently, the most meaningful measurements were made on the more stable surfaces which had been aged at high temperatures in a vacuum.

PRINCIPLES OF THE EXPERIMENTAL METHOD

The differential equation of heat flow in an electrically heated ribbon of conducting metal is given by

$$I^2 R = IE = -A \frac{\partial}{\partial z} \left(K \frac{\partial T}{\partial z} \right) + DAC \frac{\partial T}{\partial t} + \epsilon_H P \sigma T^4 - \alpha P \sigma T_0^4$$

where I is the current; R , the resistance per unit length; E , the voltage per unit length; z , the distance along the ribbon; A , the cross-sectional area; K , the thermal conductivity; T , the absolute temperature; D , the density; C , the heat capacity; ϵ_H , the total hemispherical emittance; P , the radiating area per unit length; σ , the Stefan Boltzmann constant; and α is the absorptivity of the ribbon at temperature T for radiation with a relative spectral distribution equal to that of a black body at the wall temperature T_0 .

The terms on the left side of this equation represent the power generated within the ribbon and are equated to the power dissipated by conduction and radiation plus the energy stored. The last term on the right is the power absorbed by the ribbon from its surroundings at temperature T_0 . This equation does not include a convective term since a vacuum environment only will be considered. It is also assumed that the walls are non-reflecting. In a steady state condition at the center of a ribbon of sufficient length to establish a uniform temperature region, the energy will be lost by radiation only. Then this equation reduces to

$$I^2 R = IE = P \alpha \left(\epsilon_H T^4 - \alpha T_0^4 \right) = \epsilon_H P \alpha \left(T^4 - \frac{\alpha}{\epsilon_H} T_0^4 \right)$$

It is often found that α/ϵ_H is arbitrarily set equal to one, or that the term $\alpha T_0^4/\epsilon_H$ is neglected altogether. The omission of the term will account for an error which is less than one percent when T/T_0 is equal to three or greater, but if $T_0 = 300^\circ \text{K}$ an appreciable error may occur when dealing with ribbons at temperatures much less than 1000°K . When $\alpha T_0^4/\epsilon_H$ is taken into account, the problem arises as to what value to attach to α/ϵ_H .

The spectral absorptivity is equal to the spectral emissivity. Thus, the absorptivity of the ribbon at temperature T is given by

$$\alpha_\lambda = \epsilon_\lambda = 2 \left(\frac{\rho}{30\lambda} \right)^{1/2} - 2 \left(\frac{\rho}{30\lambda} \right) + 2 \left(\frac{\rho}{30\lambda} \right)^{3/2} + \dots$$

where ρ is the electrical resistivity in ohm-cm and λ is the wavelength in centimeters. When this is multiplied by the Planckian distribution of the impinging wall radiation at temperature T_0 , and integrated over all wavelengths, it is found that

$$\alpha = 0.754(\rho T_0)^{1/2} - 0.635(\rho T_0) + 0.673(\rho T_0)^{3/2} + \dots$$

where ρ is the electrical resistivity at temperature T , while the total hemispherical emittance is given by equation (2). Hence,

$$\frac{\alpha}{\epsilon_H} = \frac{0.754(\rho T_0)^{1/2} - 0.635(\rho T_0) + \dots}{0.754(\rho T)^{1/2} - 0.635(\rho T) + \dots}$$

and in the limit of low values of ρT ,

$$\frac{\alpha}{\epsilon_H} \approx \left(\frac{T_0}{T} \right)^{1/2}$$

so that

$$I^2 R = IE = \epsilon_H P \sigma \left[T^4 - \left(\frac{T_0}{T} \right)^{1/2} T_0^4 \right] \quad (3)$$

This is an approximate correction and should be relied upon only when the magnitude of the correction is still quite small. When the voltage per unit length and the current are known, both the resistivity and total hemispherical emittance may be found.

Thus,

$$\rho = \frac{EA}{I} \quad (4)$$

and from equation (3)

$$\epsilon_H = \frac{IE}{P \sigma \left[T^4 - \left(\frac{T_0}{T} \right)^{1/2} T_0^4 \right]} \quad (5)$$

The total normal emittance may be determined with a thermopile that has been calibrated for black body radiation by comparing the normal power of the specimen relative to that of a black body at the same temperature. Thus the total normal emittance is

$$\epsilon_N = \frac{Bx \pi}{\sigma \left[T^4 - \left(\frac{T_0}{T} \right)^{1/2} T_0^4 \right]} \quad (6)$$

where B is the thermopile calibration constant and x is the thermopile output voltage. The product Bx is numerically equal to the normal radiated power in watts per cm² per unit solid angle.

Now the ratio of total hemispherical to total normal emittance may be arrived at by two methods. First, by the quotient of the emittances from equations (5) and (6) and second, by measuring the angular distribution of radiation from a plane surface. The ratio by the first method is

$$\frac{\epsilon_H}{\epsilon_N} = \frac{EI}{PBx\pi} \quad (7)$$

The calculation of this ratio by the latter method is based on the following derivation. The total radiant power emitted into a hemisphere per unit area is

$$H = \epsilon_H \sigma T^4 = \int_0^{\pi/2} \epsilon_N \frac{\sigma T^4}{\pi} f(\theta) 2\pi \sin\theta d\theta \quad (8)$$

where $\epsilon_N \sigma \frac{T^4}{\pi}$ is the power emitted per unit solid angle normal to the surface, $f(\theta)$ is the ratio of the intensity at angle θ to the normal intensity and $2\pi \sin\theta d\theta$ is the differential solid angle. When the assumption is made that the emitting surface is Lambertian, then $f(\theta) = \cos\theta$, but this is not valid in the case of polished metals.¹ The expression for the ratio of total hemispherical to total normal emittance may then be written

$$\frac{\epsilon_H}{\epsilon_N} = 2 \int_0^{\pi/2} f(\theta) \sin\theta d\theta = 2 \int_0^1 f(\theta) d(\cos\theta)$$

This may be numerically integrated in the form of the sum

$$\frac{\epsilon_H}{\epsilon_N} = 2 \sum_{n=1}^S f(\theta_n) (\cos\theta_n - \cos\theta_{n+1}) = \frac{2}{S} \sum_{n=1}^S f(\theta_n) \quad (9)$$

where S is the number of equal increments along the $\cos\theta$ axis between 0 and 1, and the θ_n are chosen such that the $\cos\theta_n$ are separated by equal increments of $1/S$, and $f(\theta_n)$ is the ratio of the intensity at θ_n to the normal intensity.

Since the interest here is only in relative intensity, no absolute calibration of the detector is necessary as in the case where the detector is used for direct determination of normal emittance.

The spectral emittance at 0.65 micron may also be readily determined if the true temperature and brightness temperature of the ribbon are known.

On the basis of Wien's law the following relation is established:

$$\epsilon_{\lambda} \exp (-c_2/\lambda T) = \exp (-c_2/\lambda T_A)$$

where T is the true temperature of the ribbon and T_A is the brightness temperature. This reduces to

$$\epsilon_{\lambda} = \exp \left[-2.214 \times 10^4 \left(\frac{T - T_A}{T T_A} \right) \right] \quad (10)$$

where $\lambda = 0.65\mu$ and $c_2 = 1.4388$. Therefore, the total hemispherical emittance, total normal emittance, spectral emittance, and resistivity of a conducting ribbon may be found if the true temperature, apparent temperature, current, voltage per unit length, and angular distribution of emitted energy are known.

EXPERIMENTAL ARRANGEMENT

The experimental arrangement is shown in Figures 1 and 2. The sample under test is in the form of a ribbon either 12 or 6 in. long, 1 cm wide, and 0.005 in. thick. The ribbon is supported vertically in a chamber where a vacuum is maintained at from 3×10^{-7} to 10^{-5} Torr depending on the temperature of the sample. The lower support of the ribbon is so arranged that it may be moved vertically to compensate for thermal expansion of the specimen while being rigidly held about a vertical axis. This vertical movement is accomplished by adjustment of a tension spring device attached to the lower arm. The adjustment may be made during operation by a shaft rotating in a vacuum feed-through. The choice of either a 12 in. or 6 in. ribbon determines the length of the upper ribbon support which is interchangeable. Figure 1 shows a 6 in. ribbon installed. The ribbon clamps and support arms are force water cooled. The ribbon and its support assembly are capable of being rotated through an angle of about 200 degrees. A precision gearing system with 0.2 degree resolution induces rotation to the ribbon through a vacuum feed-through. A supplementary electronic readout system allows either visual or printed digital indication of the ribbon angle. Cooling water to the rotating ribbon support flows through spiraled Viton A tubing. The sample receives its power through a spiraled fine strand 4/0 copper conductor.

The alternating current for heating the ribbon is supplied from a 15 KVA, continuously variable, 0 to 70 volt, 1 percent voltage regulated supply. The current is determined by sensing the voltage drop across

either a 50, 100, or 200 amp shunt. For higher currents the shunts may be used in parallel. The voltage per unit length is measured within the uniform temperature region by fine tungsten (0.005 in.) wires attached to the sample a few centimeters apart. Both voltage and current information is converted to d.c. by means of a converter and then measured with a digital voltmeter allowing both visual and printed read-out. Thermocouples are attached to the ribbon for temperature sensing; a complete description of the temperature measuring technique will follow in a subsequent section.

The thermopile consists of the element from a Minneapolis-Honeywell Radiamatic pyrometer enclosed in a water cooled brass housing. The element has 10 iron-constantan junctions in a circular configuration about 3mm diameter. The field of view of the thermopile at the ribbon plane is about 2 cm wide and 1-1/2 cm along the ribbon axis. This field of view is within the uniform temperature region of the ribbon. Thus the area of the ribbon within the field of view decreases as the cosine of the angle from the normal as the ribbon is rotated. If a sample were radiating from a perfectly diffuse (Lambert) surface, then the radiant energy received by the thermopile would decrease as the cosine of the angle from the normal as does the projected area. This is the basis for being able to measure the ratio of total hemispherical to total normal emittance of a non-diffuse surface since the energy received does not fall off as the cosine of the angle (see Figure 15). To measure the total normal emittance directly, an absolute calibration of the thermopile was accomplished by measuring the angular distribution of radiation from a tantalum ribbon over a wide range of energies. Then, using equations (5), (6), and (9) we determined B, the calibration constant. The calibration was checked by observing the radiation from a cylindrical graphite rod. Here it was necessary to assume that $\epsilon_M/\epsilon_N \approx 1$ for graphite. Based on published information, this is not an unreasonable assumption. Figure 3 is the calibration of the thermopile with B being the slope of the line. The ordinate is the power radiated per square centimeter from a 1 cm wide ribbon into a unit solid angle normal to the ribbon. The abscissa is the deflection in millivolts as indicated on the thermopile amplifier. A solenoid-operated shutter is incorporated as part of the thermopile so that a zero may be obtained. Besides the radiating ribbon, the thermopile sees only the grooved water cooled plate (see Fig. 1) behind the ribbon. The plate is blackened with platinum black and is at the same temperature as the thermopile cold junctions.

The whole assembly is enclosed within an 18 in. diameter aluminum vacuum chamber. The chamber is cooled by cold water flowing through copper tubing fastened to the walls with heat conducting cement (see Figure 2). A liquid nitrogen cooled chevron baffle lies between the diffusion pump and the chamber itself. This serves as a cold trap as well as a way to prevent the back-streaming of the diffusion pump oil. The pressure is monitored with a Bayard-Alpert type ionization gauge. The lowest pressure attained after long chamber outgassing was 3×10^{-7} Torr; however, the

routine pressures are about 1 to 2×10^{-6} Torr at low sample temperatures. At high sample temperatures the pressure is roughly equivalent to the vapor pressure of the sample itself at early measurement times. If the high temperature is held for longer periods of time, those internal components not water cooled would outgas as they warmed. No measurements were made at pressures greater than 1×10^{-5} Torr.

TEMPERATURE DETERMINATION

Since the total hemispherical emittance is roughly proportional to the temperature, the radiant energy emitted by a polished metal surface is proportional to about the fifth power of temperature through the equation $H = \epsilon_{\text{H}} \sigma T^4$. This places the temperature as by far the most important variable in any radiation transfer problem. Unfortunately its importance is only exceeded by its difficulty of measurement, particularly in the region above 1800°K . With the excellent success obtained with platinum thermocouples up to 1800°K in previous phases of this project, it was naively assumed that a nearly similar success would be forthcoming when refractory metal thermocouples (tungsten-tungsten, 26 percent rhenium) were used to extend the upper temperature limit to 3000°K . This assumption was soon shattered when the accuracy and reproducibility were found to be far below that necessary for emittance measurements that could be viewed with confidence.

Tungsten-tungsten, 26 percent rhenium thermocouples 0.005 in. diameter (hereafter noted as W-W/Re) were obtained from two manufacturers. The first obtained was supplied with a calibration up to 2800°C (call these type A). The second was supplied with a notary certified calibration up to 2300°C (call these type B). The type A thermocouple was tried initially on a tantalum ribbon. The wires were attached by drilling 0.005 in. holes in the center of the ribbon about 2 mm apart, inserting the wires through the holes a short distance, and then squeezing the wire by peening the ribbon around the wire with the aid of a punch with rounded nose and a center hole to accommodate the end of the wire. Excess wire was then clipped off. Measured total and spectral emittance values were found to be completely unrealistic. Also after trying the same configuration on subsequent ribbons of the same material the emittances were found to be not only unrealistic but also not reproducible.

Upon receipt of type B thermocouples, the same problem was encountered; however, in this case the emittance values up to 2000°K appeared at least reasonable although some non-reproducibility was still noted. Some ribbons were then instrumented with both type A and type B W-W/Re thermocouples, as well as a platinum-platinum, 10 percent rhodium thermocouple. Up to 1800°K type B agreed reasonably well with the platinum couple, while type A deviated considerably. Emittances calculated from the platinum measured temperature were quite within expectation.

It was evident that a complete calibration must be undertaken before the W-W/Re couples could be used. A tantalum cylinder $3/4$ in. in diameter by $1/2$ in. deep was instrumented with type A and type B W-W/Re couples. Also, two platinum-platinum, 10 percent rhodium couples, one a 0.005 in. working thermocouple and the other a 0.008 in. calibrated standard were also used. Black body holes 0.016 in. were drilled at various places in the surface. The assembly was placed in the coil of an induction heater and compared in vacuum up to 1800°K . A micro-optical pyrometer was used to monitor the temperature in the black body holes. The pyrometer temperature, the two platinum couples, and the type B W-W/Re thermocouple agreed well within ± 1 percent over this range, while type A deviated as much as 80°C . The platinum couples were then removed and the comparison extended to the power limit of the furnace -- 2100°K . Type B and the pyrometer remained within ± 1 percent while type A did not compare. Although the temperature limit was nowhere near the 3000°K desired nor the thermocouples tested in their normal mode of operation (attached to the ribbon), this calibration at least eliminated one of the thermocouples as not suitable for further testing.

In order to calibrate the thermocouples in their normal mode of operation, it was necessary to use the spectral emittance of tantalum as an intermediate step. A tantalum ribbon, 1 cm wide, 6 in. long, and 0.005 in. thick was folded the long way into a triangle with sides approximately $1/3$ cm. The closed length of the triangle was about 4 in. Several 0.005 in. and 0.010 in. holes were drilled into one side to serve as black body holes. The triangle was instrumented with type B W-W/Re thermocouples and aged at 2400°K for 15 minutes. Measurements of true temperature, brightness temperature of the tantalum surface, and thermocouple output voltage were made from 1000°K to 2800°K . The true temperature was obtained by sighting the optical pyrometer at the black body holes; the brightness temperature of the surface was taken adjacent to the holes. The resulting spectral emittance at 0.65 microns may be seen in Figure 6. The upper temperature limit was set by the evaporation of the tantalum above 2800°K with subsequent viewing port coating preventing further optical pyrometer observations. A calibration was also obtained for the attached thermocouple, although another check was still necessary in their normal mode of operation.

As an added complication, two identical micro-optical pyrometers, one recently acquired, the other on hand for 2 years or more, were compared and found to be as much as 1 percent different in their indicated temperature. The error was largest in the range 1800°C to 2200°C . Below this temperature they were nearly identical in calibration. Above this range there was an error but not as serious. A more exact calibration is planned for the immediate future.

Another 6 in. section of the ribbon identical to that formed into the triangle was instrumented and aged as before; however, this time the section was used as a flat ribbon. Brightness temperature data from the triangle were used to obtain the true temperature and the thermocouple was again

calibrated with results nearly identical to the previous measurement. Hence a calibration was obtained for type B W-W/Re thermocouples from 1000°K to 2800°K in their normal mode of operation. It should be pointed out here that the previously mentioned non-reproducibility of emittance data was essentially eliminated by adopting one thermocouple attachment technique out of the many tried that gave reproducible results. This consisted of inserting the thermocouple wire through the hole in the ribbon then spreading the end of the wire slightly and pulling the wire vigorously back into the hole. The wedging was sufficient to hold the wire and the attachment eliminated the ribbon deformation previously necessary in peening. Results of many measurements confirm the reproducibility of this method. The calibration was within ± 1 percent of that supplied with type B thermocouple up to 2150°K. Above this the deviation became extreme (90° difference at 2600°K). In the following description of results, the over-all temperature accuracy is estimated to be within ± 1 percent to 2800°K and ± 1.5 percent from 2800°K to 3000°K. The range from 2800°K to 3000°K was obtained by various means of extrapolation. Measurements on tungsten, described in the following section, added confidence to this extrapolation.

RESULTS

Due to the difference in behavior between the various metals studied as related to their environmental conditions, the results are presented separately for each metal. Data are included on the electric resistivity versus temperature on the materials studied; however, it should be noted that due to the inability to accurately determine the effective cross-sectional area of the ribbon between the voltage probes, resistivity data are normalized at low temperatures to the most frequently published value of resistivity. The resulting curves are then just the relative variation of resistivity with temperature. These are used as a check on the experimental performance of the system as well as for calculating theoretical emissivity values derived from equations (1) and (2).

Tantalum

The total hemispherical emittance and the total normal emittance versus temperature are presented in Figure 4. The data points for the hemispherical emittance represent measurements from four different samples, using both brightness temperature and thermocouple data to determine emittance. At low temperatures tantalum exhibits a gettering action for gases in the vacuum system, with a subsequent change in the hemispherical emittance. This can be seen as the short dashed line between 1200°K and 1500°K. If the emittance is measured on a fresh unaged tantalum ribbon it will follow the dashed line to about 1500°K where the gases will be

driven off, resulting in a sudden drop in the emittance to the solid line. Measurements above this temperature appear quite stable. If after aging, measurements are made below 1500°K with dispatch, then the solid line is the result. However, if a temperature below 1500°K is maintained for an extended period the emittance returns to the dashed line (rate depends on pressure). The gas sorption and liberation can be noted on the vacuum gauge connected to the measuring chamber. A separate study of emittances is advised for those interested in long term heat transfer properties below 1500°K.

The total normal emittance shown in Figure 4 is determined from angular distribution measurements every 300°K from 1200°K to 2400°K. Figure 5 is a graph of the ratio of total hemispherical to total normal emittance versus temperature. During the time that angular distribution measurements were being made on tantalum, the thermocouple had not yet had an absolute calibration check so that no total normal emittance values were determined based on absolute normal radiation as in equation (6). The spectral emittance at 0.65 microns is determined from equation (10) with the aid of true and brightness temperatures acquired during the triangle thermocouple calibration and plotted versus temperature in Figure 6. Figure 7 shows the electrical resistivity versus temperature curve normalized at 1100°K to the data of Malter and Langmuir.⁷

Niobium

A gettering action similar to that observed with tantalum is exhibited by niobium except that the transition or outgassing temperature of the latter appears to be 1400°K. This can be seen in Figure 8 which is a plot of total hemispherical and total normal emittance versus temperature up to 2400°K. Evaporation made measurements above this temperature prohibitive. The total normal emittance was determined from calibrated thermopile measurements and equation (6). The ratio of total hemispherical to total normal emittance is determined from equation (7) and plotted versus temperature in Figure 9. True temperatures for the niobium measurements were determined with the thermocouples calibrated as previously described. Figure 10 is a display of the spectral emittance at 0.65 microns versus temperature and Figure 11 is a plot of electrical resistivity versus temperature normalized at 1200°K to the data of Ames and McQuillan.⁸

Tungsten

Considerable effort has been expended by other investigators in the past on the thermal radiation properties of tungsten with much of the

impetus coming from its use by the lighting industry. Consequently, the relation between brightness and true temperature as determined by Roeser and Wensel, and shown in Gubareff's work,⁹ has been used to obtain the true temperature in this research. Concurrently, however, the calibrated type B W-W/Re thermocouple was also used. The total hemispherical emittance, which is quite sensitive to temperature differences, has about ± 5 percent spread using both temperature measuring techniques as can be seen in Figure 12. The emittance determined with the brightness temperature appears generally to be a few percent higher in the middle and upper temperature regions as indicated by the data points with circles. Considering the problems associated with the thermocouples at high temperatures, and the non-equivalence of the tungsten surface between this investigation and that of Roeser and Wensel, this is not a surprising difference. The uncertainty in optical pyrometer temperatures in the vicinity of 2100°K as pointed out in the section on temperature determination could contribute to the wider spread in this region. The reasonable agreement in the two techniques was the basis for using brightness temperature data to help extrapolate the thermocouple calibration from 2800°K to 3000°K. The tungsten samples used were aged at 2400°K for approximately 30 minutes. The total normal emittance shown in Figure 12 was determined with the calibrated thermopile and equation (6).

Figure 13 shows the ratio of total hemispherical to total normal emittance (from equation (7)) versus temperature. Figure 14 is a display of electrical resistivity versus temperature normalized at 1400°K to the data of Jones and Langmuir.¹⁰

DISCUSSION

Part of the original viewpoint underlying this research was that the sample surfaces should be as highly polished and accurately characterized as possible. However, it was found that aging at high temperatures until equilibrium was reached in the appearance of the surface geometry, created a surface nearly independent of preaging preparation. In the "as received" condition, all the samples used were smooth rolled, some quite specular, others slightly dull in appearance depending on the metal itself or the supplier. Microscopic inspection after aging revealed a prominent grain structure which appeared the same whether the ribbon had been prepolished or not. The individual grains were highly specular with boundaries sharply defined. Hence, the data presented in this report represent surfaces that are in a recrystallized condition except some of the measurements where the gettering properties of tantalum and niobium were investigated.

To provide a clearer picture of the angular radiative properties of metal, the angular distribution of radiation of molybdenum at 1210°K is

reproduced from the previous report.² Figure 15 is the intensity relative to the normal plotted against the angle from the normal. Figure 16 is the intensity relative to the normal plotted against the cosine of the angle from the normal. The departure from Lambert's cosine law is clearly evident in these figures. In Figure 16 the ratio of total hemispherical to total normal emittance can be visualized easily as the area under the experimentally observed curve. The area defined by the straight line segment is equal to unity. The ratio of total hemispherical to total normal emittance determined from angular distribution measurements on tantalum in this report was obtained by numerical integration. Consequently, the distribution was not plotted as in Figures 15 and 16.

It is often of interest to present the data on the radiative properties of all the materials studied on the same graph. Figure 17 through Figure 20, therefore, include on each graph composite information on tantalum, niobium, tungsten, and molybdenum. The data on molybdenum are taken from the previous report.²

Figure 17 is the total hemispherical emittance versus temperature. The similarity in the emittance versus temperature relation of the four metals shown in Figure 17 is the basis for the representation of the emittance by the empirical equation:

$$\epsilon_H = 0.1069 \left(\frac{T}{1000} \right)^{1.21} - 0.000926 \left(\frac{T}{1000} \right)^{4.25}$$

where T is the temperature in degrees Kelvin. The equation holds within ± 5 percent for molybdenum and tantalum from 1000°K to the evaporation limited temperature, and for niobium and tungsten from 1200°K to the evaporation limited temperature.

Figure 18 is the ratio of total hemispherical to total normal emittance versus temperature. Figure 19 is the ratio of total hemispherical to total normal emittance versus total normal emittance. The theoretical curve is obtained from equations (1) and (2). Figure 20 is the total hemispherical emittance plotted against $(\rho T)^{\frac{1}{2}}$ where ρ is the experimental value of the normalized resistivity at temperature T. The theoretical curve is from equation (2) which is repeated on the figure. Data on platinum¹ are also included in this figure. Figure 21 is the relation between brightness temperature in degrees centigrade and the true temperature in degrees Kelvin at 0.65 microns, included as a tool for true temperature determination. The curve for tungsten is from data of Roeser and Wensel although confirmed within experimental accuracy in this research.

Examination of Figure 20 clearly indicates that equation (2) does not accurately predict the total hemispherical emittance of polished metals. In all probability some of the deviation can be attributed to

the lack of equivalence between real and ideal surfaces. However, in general, surface defects tend to raise the total emittance at a given (ρT) . This effect is more pronounced at lower values of (ρT) , and would not account for the low values of ϵ_H at low values of (ρT) .

The over-all accuracy of the data is estimated to be ± 5.0 percent or better. Some of the measurements of the independent variables such as voltage, current, and certain dimensions are much better than ± 1 percent. The temperature accuracy as stated before is about ± 1 percent over most of the temperature range.

With experimental data of this type as a guideline for a more detailed accounting of electronic relaxation time, internal photoelectric effect, bound electrons, and other short wavelength phenomenon, it is hoped that a workable theory may be generated which would accurately describe the radiative properties of electrical conductors at high temperatures.

REFERENCES

1. G. L. Abbott, N. J. Alvares, and W. J. Parker, "Total Normal and Total Hemispherical Emittance of Polished Metals," USNRDL, WADD-TR-61-94, Part I, November 1961.
2. G. L. Abbott, N. J. Alvares, and W. J. Parker, "Total Normal and Total Hemispherical Emittance of Polished Metals," USNRDL, WADD-TR-61-94, Part II, January 1963.
3. E. Aschkinass, Ann. Phys. Lpz. 17, 960 (1905).
4. P. D. Foote, Bull. Nat. Bur. Stand. 11, 607 (1914/1915).
5. G. G. Gubareff, J. E. Janssen, and R. H. Torborg, "Thermal Radiation Properties Survey," 2nd Edition, page 8, Honeywell Research Center, 1960.
6. C. Davisson and J. R. Weeks, J. Opt. Soc. Amer. 8, 581 (1924).
7. L. Malter and D. B. Langmuir, Phys. Rev., 55, 743, 1939.
8. S. L. Ames and A. D. McQuillan, Resistivity-Temperature-Concentration Relationships in the System Niobium-Titanium, Acta. Met. 2, 831, 1954.
9. Same as Reference 5, page 181.
10. Jones and Langmuir, Handbook of Chem. and Phys., 32nd Edition, page 2449, 1951.

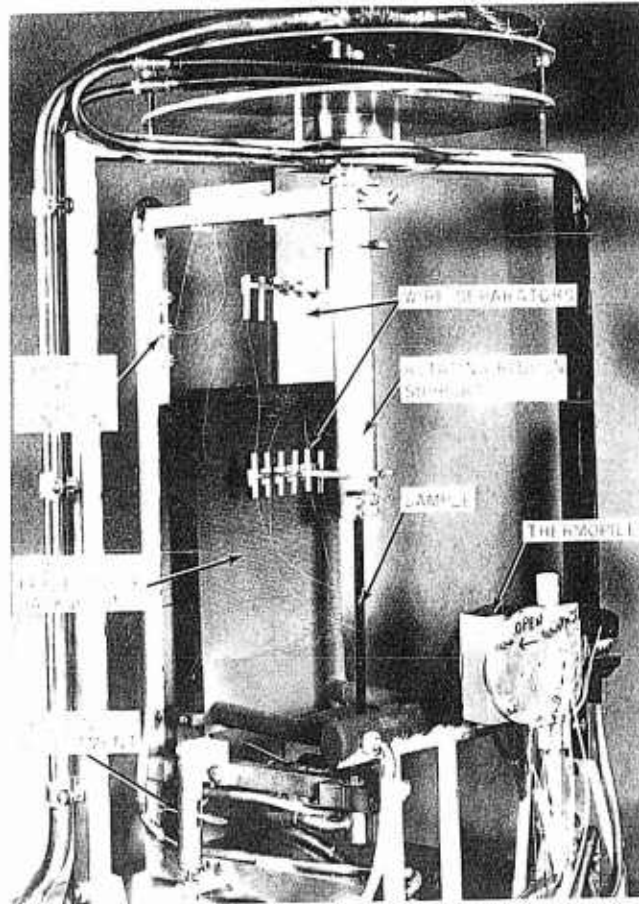


Fig. 1 Detailed Photograph of Experimental Apparatus



Fig. 2 Over-all Photograph of Experimental Apparatus

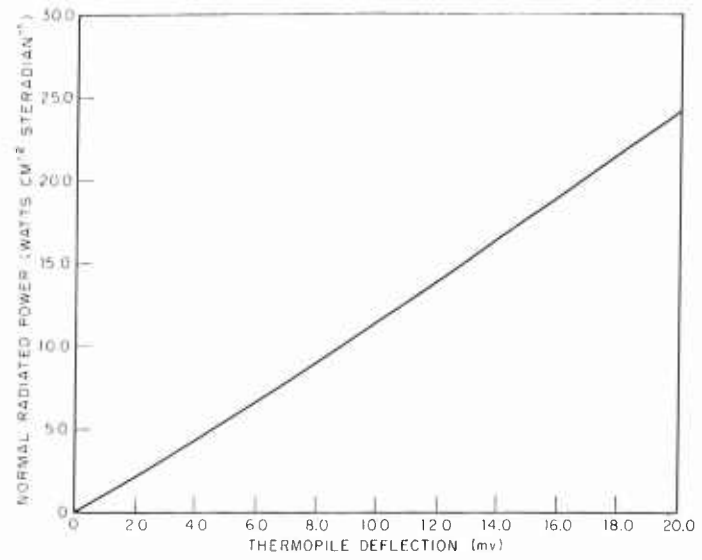


Fig. 3 Calibration Curve of Thermopile

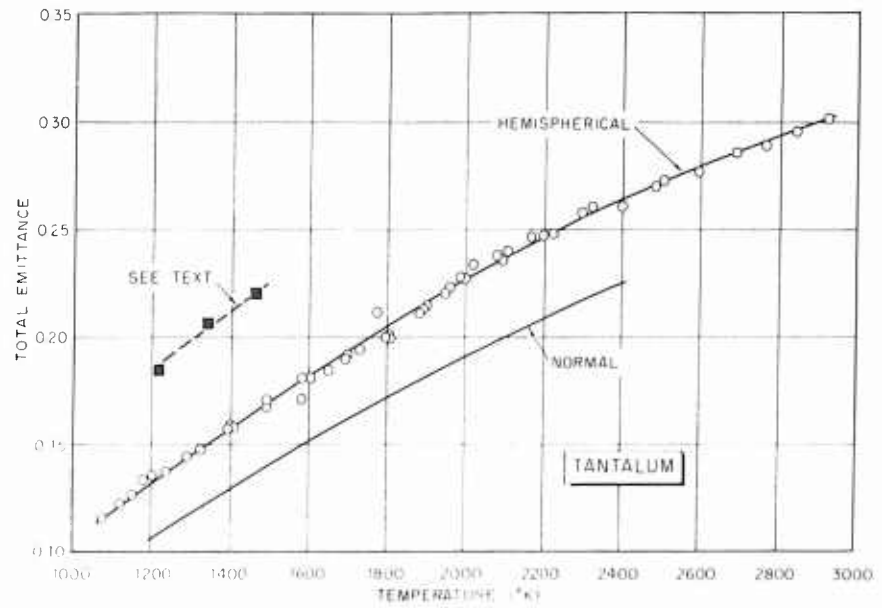


Fig. 4 Tantalum - Total Hemispherical and Total Normal Emittance

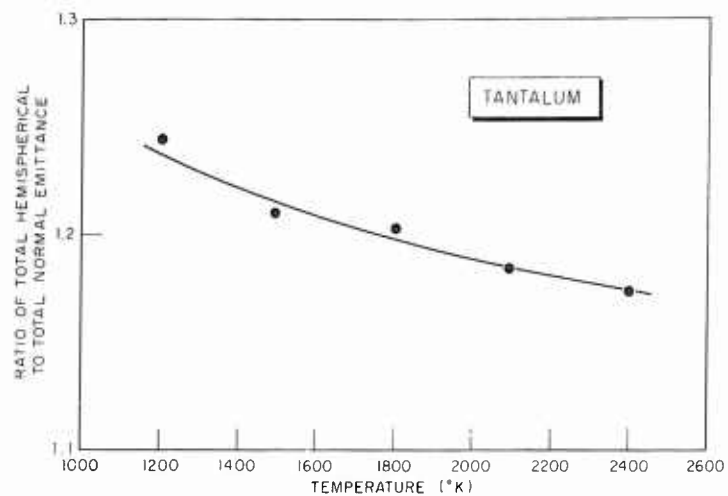


Fig. 5 Tantalum - Ratio of Total Hemispherical to Total Normal Emittance

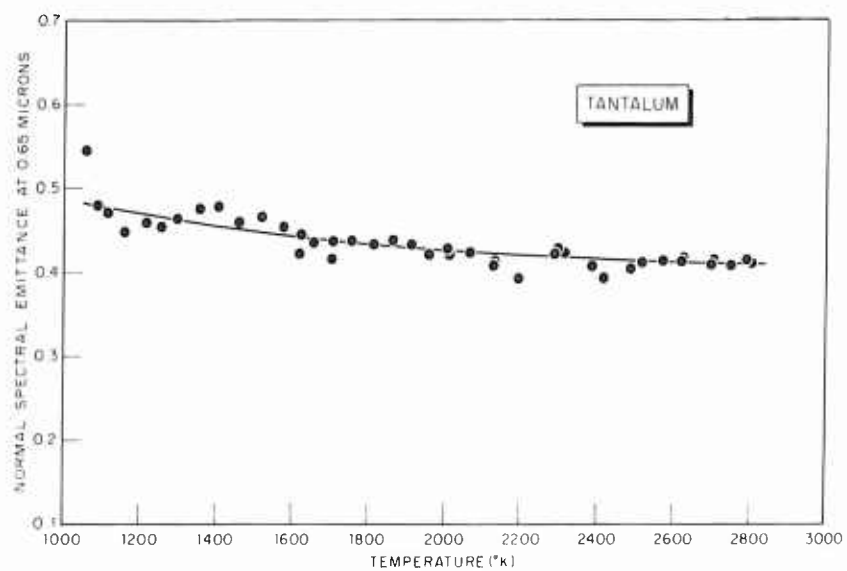


Fig. 6 Tantalum - Normal Spectral Emittance at 0.65 Micron

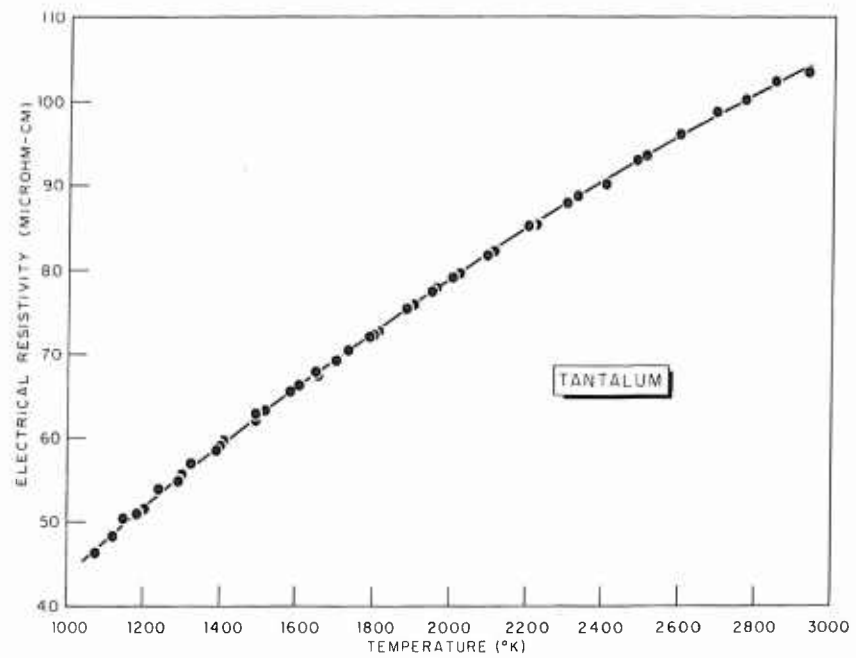


Fig. 7 Tantalum - Electrical Resistivity

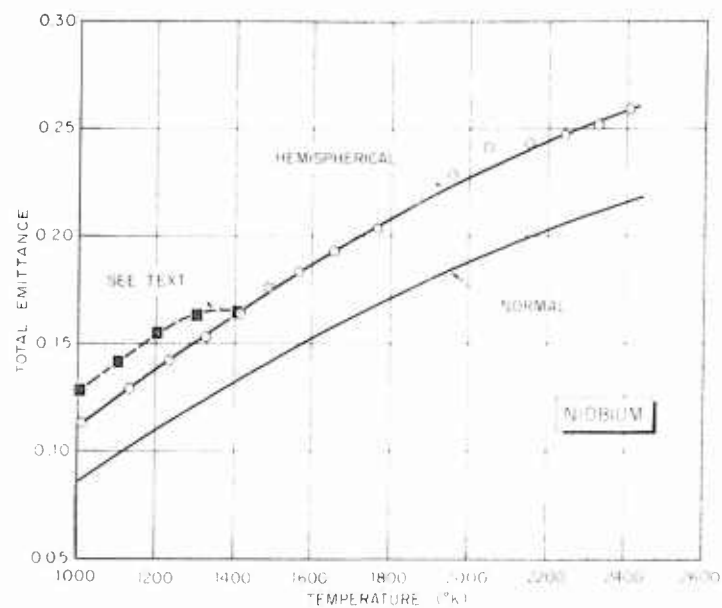


Fig. 8 Niobium - Total Hemispherical and Total Normal Emittance

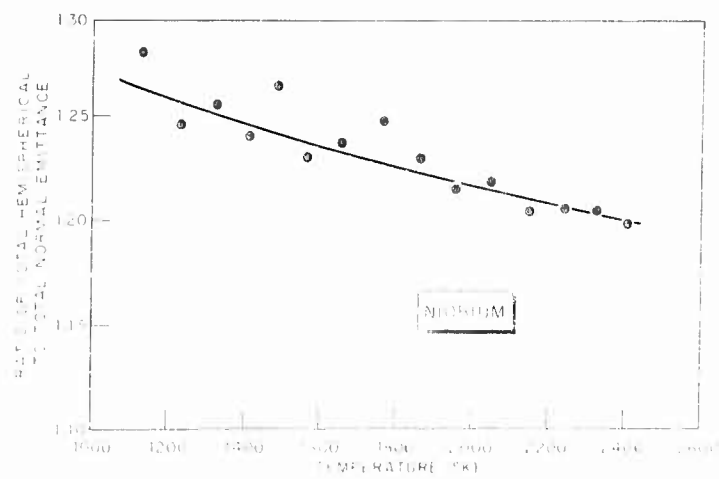


Fig. 9 Niobium - Ratio of Total Hemispherical to Total Normal Emittance

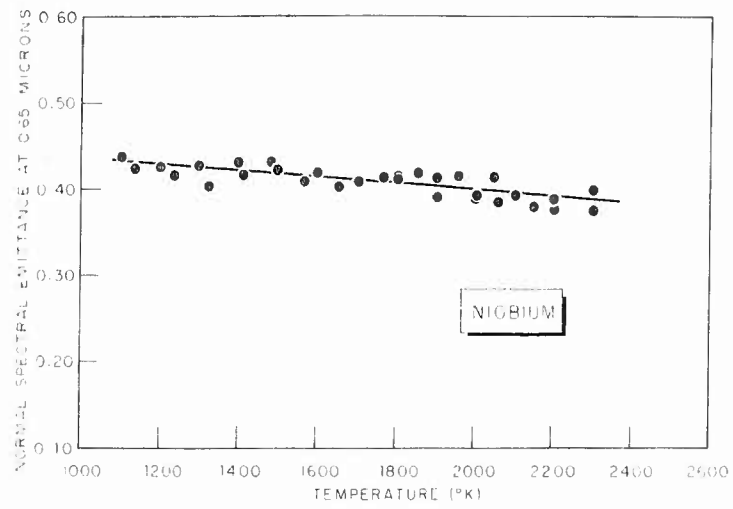


Fig. 10 Niobium - Normal Spectral Emittance at 0.65 Micron

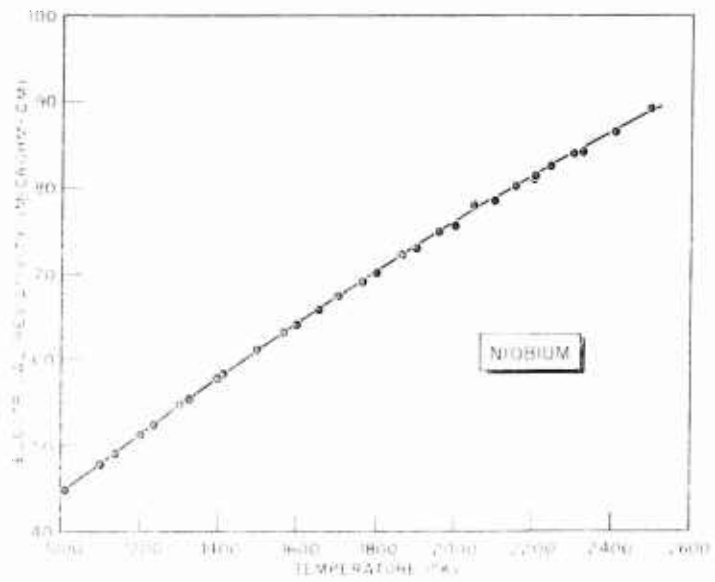


Fig. 11 Niobium - Electrical Resistivity

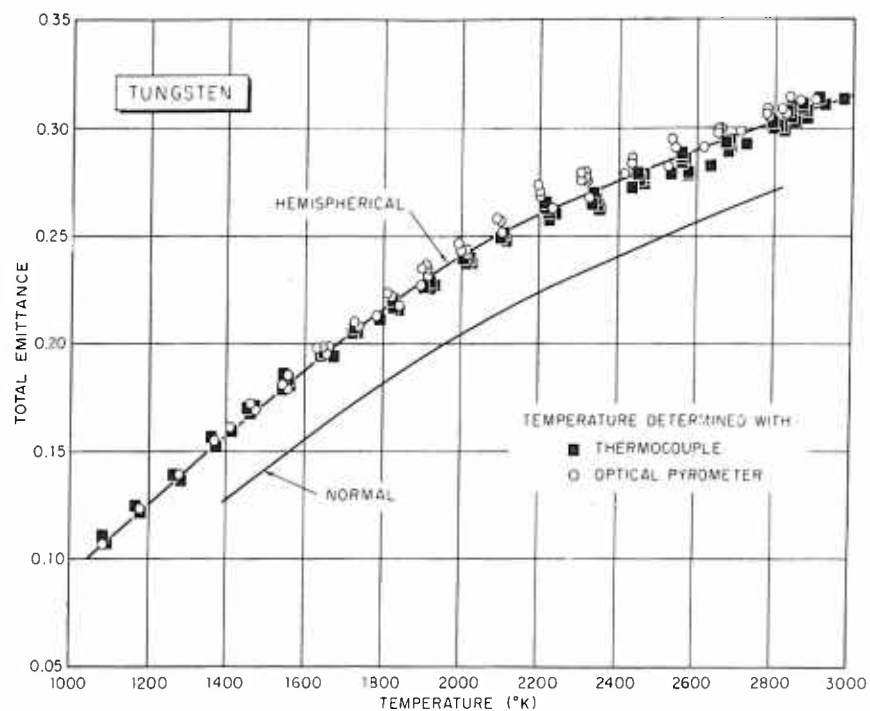


Fig. 12 Tungsten - Total Hemispherical and Total Normal Emittance

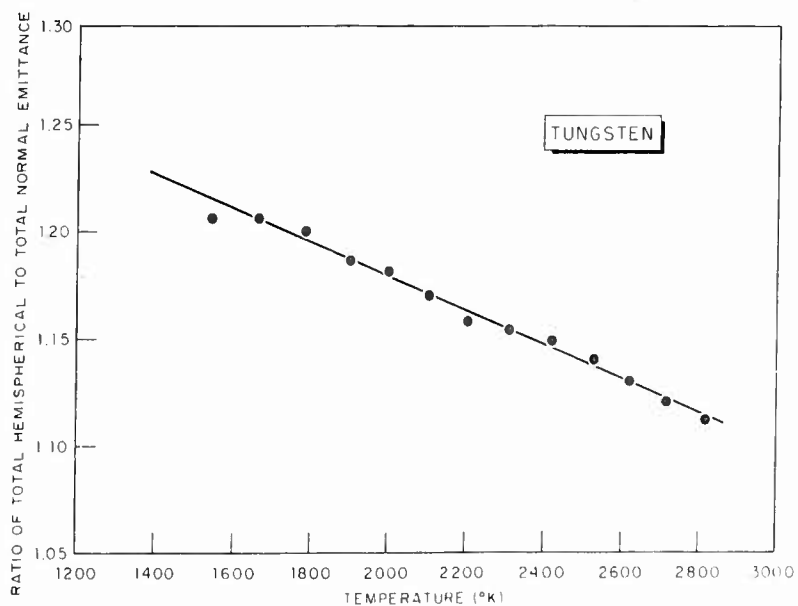


Fig. 13 Tungsten - Ratio of Total Hemispherical to Total Normal Emittance

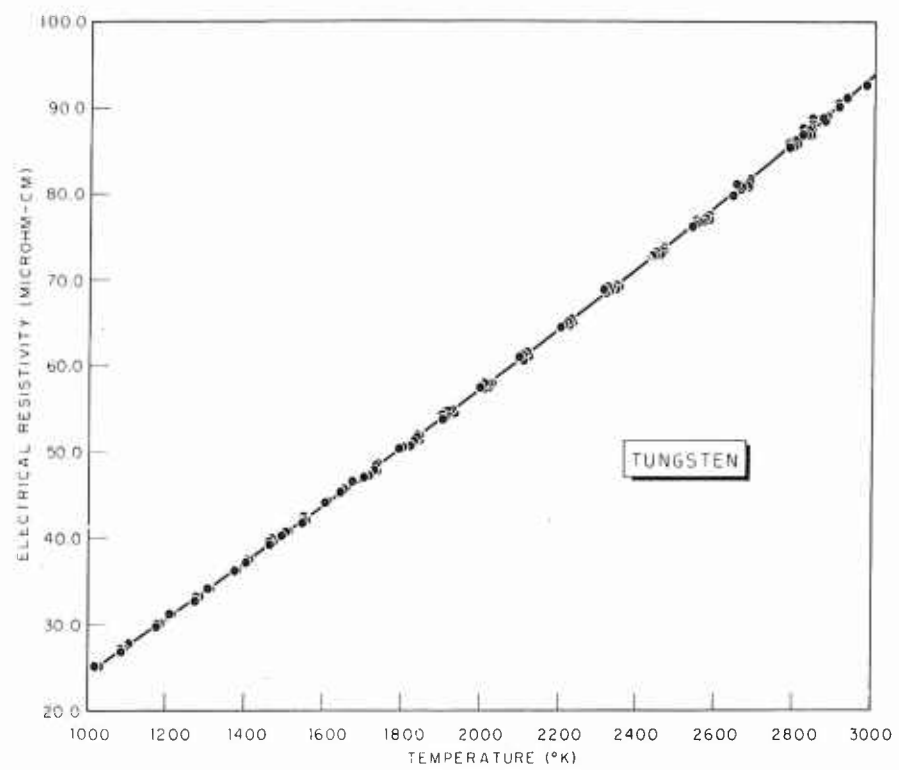


Fig. 14 Tungsten - Electrical Resistivity

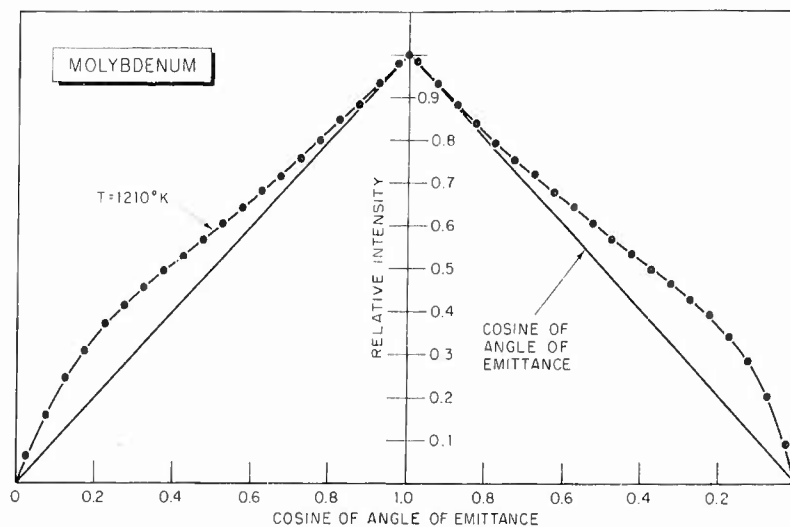


Fig. 15 Molybdenum - Angular Distribution of Radiation versus Angle from Normal

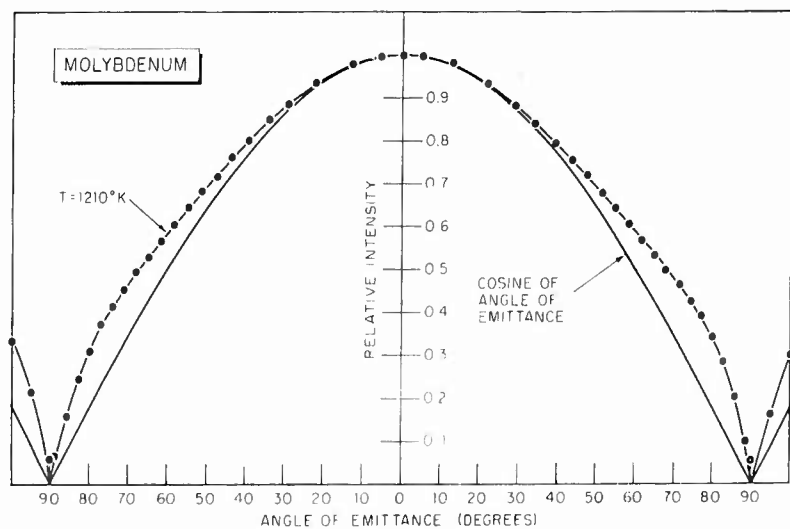


Fig. 16 Molybdenum - Angular Distribution of Radiation versus Cosine of Angle from Normal

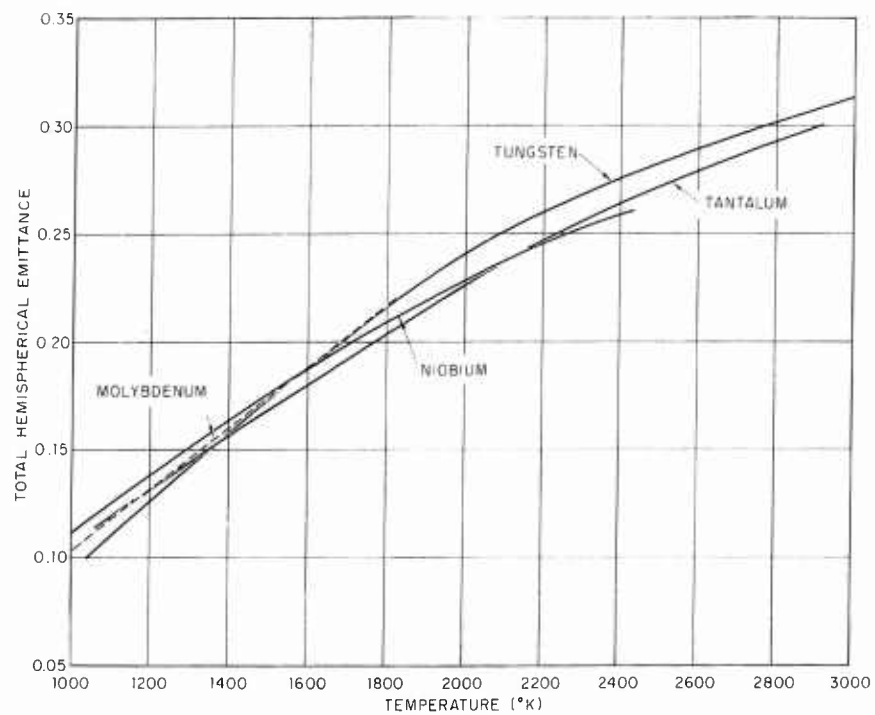


Fig. 17 Total Hemispherical Emittance of Molybdenum, Tantalum, Niobium, and Tungsten.

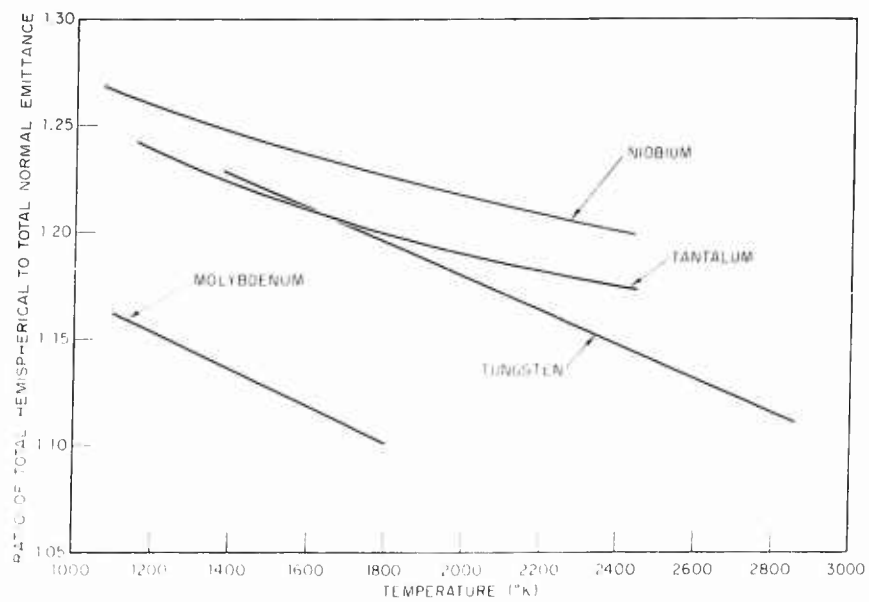


Fig. 18 Ratio of Total Hemispherical to Total Normal Emittance of Molybdenum, Tantalum, Niobium, and Tungsten.

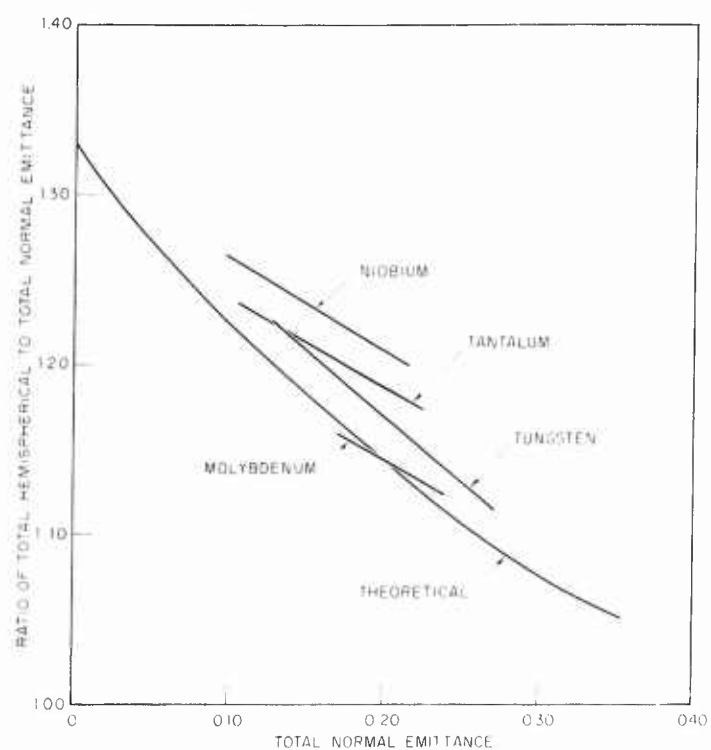


Fig. 19 Ratio of Total Hemispherical to Total Normal Emittance versus Total Normal Emittance for Molybdenum, Tantalum, Niobium, and Tungsten.

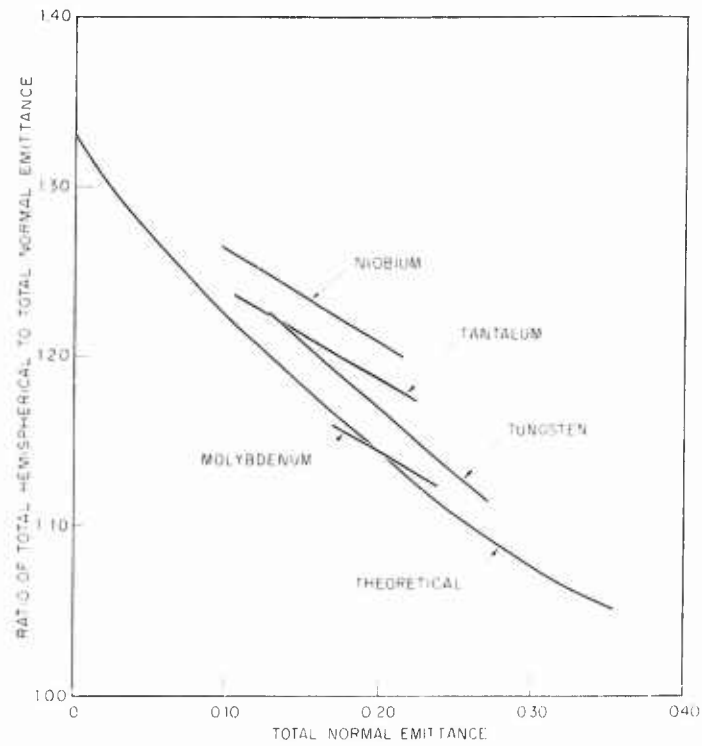


Fig. 19 Ratio of Total Hemispherical to Total Normal Emittance versus Total Normal Emittance for Molybdenum, Tantalum, Niobium, and Tungsten.

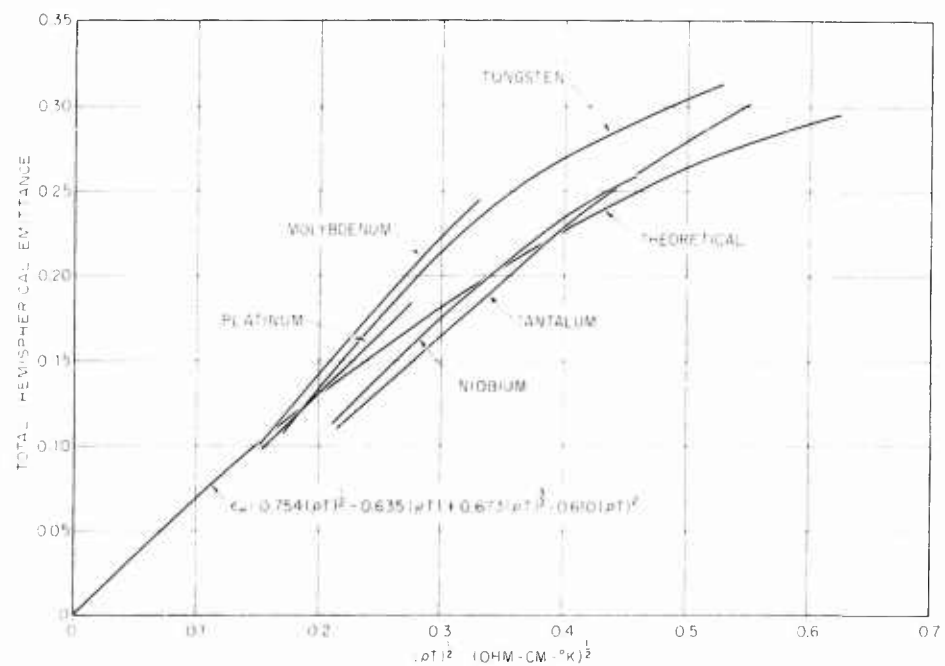


Fig. 20 Total Hemispherical Emittance of Platinum, Molybdenum, Tantalum, Niobium, and Tungsten versus the Square Root of the Product of Electrical Resistivity and Temperature.

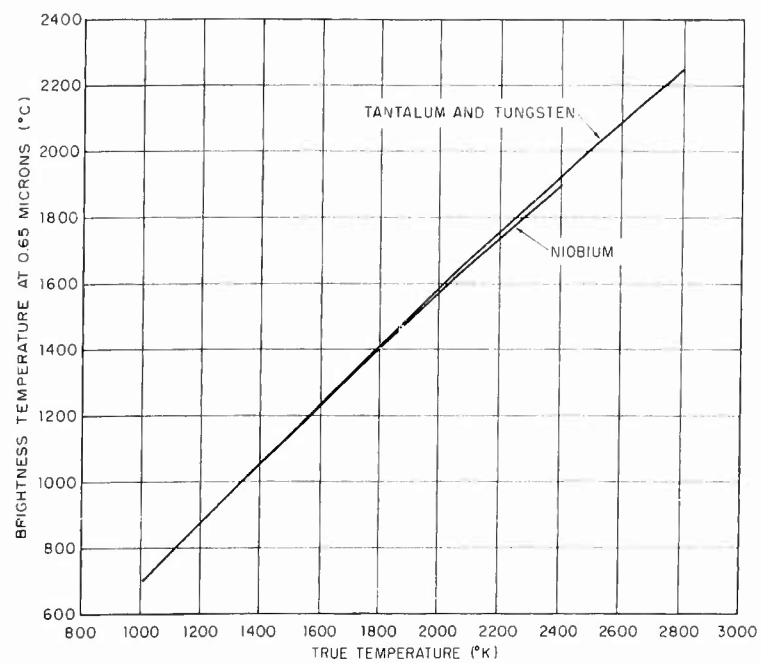


Fig. 21 Brightness and True Temperature Relationship for Tantalum, Niobium and Tungsten.